JAERI-M
86-113

POWER TEST OF THE JT-60 ICRF LAUNCHING SYSTEM

August 1986

Haruyuki KIMURA, Tsuneyuki FUJII, Yoshitaka IKEDA
Mikio SAIGUSA, Junki SAGAWA[*1], Masami SEKI
Munenori UEHARA[*2], Noriyuki KOBAYASHI[*3] and Yasushi SAITO[*3]

日本原子力研究所
Japan Atomic Energy Research Institute

JAERI-Mレポートは，日本原子力研究所が不定期に公刊している研究報告書です。
入手の問合わせは，日本原子力研究所技術情報部情報資料課（〒319-11茨城県那珂郡東海村）あて，お申しこしください。なお，このほかに財団法人原子力弘済会資料センター（〒319-11 茨城県那珂郡東海村日本原子力研究所内）で複写による実費頒布をおこなっております。

JAERI-M reports are issued irregularly.
Inquiries about availability of the reports should be addressed to Information Division Department of Technical Information, Japan Atomic Energy Research Institute, Tokai-mura, Naka-gun, Ibaraki-ken 319-11, Japan.

編集兼発行　日本原子力研究所
印　　刷　㈱高野高速印刷

Power Test of the JT-60 ICRF Launching System

Haruyuki KIMURA, Tsuneyuki FUJII, Yoshitaka IKEDA,
Mikio SAIGUSA, Junki SAGAWA*1, Masami SEKI,
Munenori UEHARA*2, Noriyuki KOBAYASHI*3 and
Yasushi SAITO*3

Department of Large Tokamak Research
Naka Fusion Research Establishment
Japan Atomic Energy Research Institute
Naka-machi, Naka-gun, Ibaraki

(Received July 14, 1986)

Impedance matching and power test of the JT-60 ICRF launching system was performed on the test stand before installation into the JT-60 vacuum vessel. Impedance matching of the 2×2 phased loop antenna array was confirmed with various phasing conditions. The antenna input impedance changes considerably according to the phasing because of the mutual coupling among the loops.

Multipactoring discharge was observed and its power region was clarified.

Rf energy of 1 MJ could be injected into the half part of the launching system after the aging of effectively 2 days. Observation of the aging

---

*1 On leave from Hitachi Ltd.

*2 On leave from Toshiba Ltd.

*3 Toshiba Ltd.

process, such as gas desorption, mass analysis, measurement of the temperature of the launcher etc., is discussed.

Keywords: JT-60, ICRF, Launcher, Impedance Matching, Phased Loop Antenna Array, Multipactoring Discharge, Aging, Gas Desorption

ＪＴ－60　ＩＣＲＦ結合系の耐電力試験

日本原子力研究所那珂研究所臨界プラズマ研究部
木村晴行・藤井常幸・池田佳隆
三枝幹雄・佐川準基[*1]・関　正美
上原宗則[*2]・小林則幸[*3]・斎藤　靖[*3]

（１９８６年７月１４日受理）

ＪＴ－60　ＩＣＲＦ結合系のインピーダンス整合及び耐電力試験がＪＴ－60本体真空容器への組込みに先立ってテストスタンドにて行われた。２行２列の位相制御型ループアンテナアレイのインピーダンス整合が種々の位相設定条件に対して確認された。ループ間の相互結合により，アンテナの入力インピーダンスは位相条件に従って大きく変化する。マルチパクター放電が観測され，そのパワー領域が明きらかにされた。実質２日間のエージングの後に，結合系の２分の１部分に１ＭＪの高周波エネルギーを注入することができた。ガス放出，質量分析，ランチャーの温度計測等，エージング過程に於ける観測結果が論じられる。

＊１　外来研究員：（株）日立製作所

＊２　外来研究員：（株）東芝

＊３　（株）東芝

Contents

目　　次

1. Introduction

This paper describes the results on the tests of the JT-60 ICRF launcher before installation into the JT-60 vacuum vessel.

The JT-60 ICRF heating experiment is the first attempt of the second harmonic heating in the large tokamak device, which is the most attractive heating regime in application of the ICRF to a fusion reactor. The current drive by the fast wave will be also tested. From the point of view of the rf heating technology, the launcher developed for high power density and long pulse operation will be tested in the reactor-like circumstances.

The basic specifications of the JT-60 ICRF heating system are as follows.

RF power	:	6 MW
Frequency	:	110 MHz ~ 130 MHz
Pulse width	:	10 sec.
Duty cycle	:	1/60
Launcher	:	2 × 2 phased loop antenna array

The detailed descriptions of the total heating system are given in Ref. 1.

The contents of the present test are twofold.

(1) Impedance Matching Test

The JT-60 ICRF launcher is a 2 × 2 phased loop antenna array. Each antenna element is connected to a double stub tuner individually, because of the phase control. The antenna elements couple mutually and its degree depends on the position of the stub tuner. Therefore, it is important to check the feasibility of the impedance matching of this launching system with simultaneous injection into all the elements.

We try the impedance matching for four types of the phasing, i.e. $(0,0)$, $(0,\pi)$, $(\pi,0)$ and (π,π), where the former is the toroidal phase

difference and the latter is the poloidal one.

(2) Power Test

The total launching system including the sub tuners is assembled on the test stand. Rf power is injected into the launching system in the vacuum condition in order to check the reliability of the launching system against high voltage and high current during 10 sec.

We can evaluate basic performance and quality of the launching system by these tests before commissioning. The contents of this paper are as follows.

In Sec. 2, brief descriptions of the JT-60 ICRF launcher and the experimental set-up on the test stand are given. The result on the impedance matching test is described in Sec. 3. Observation of the multipactoring discharge and experimental results on the aging process are prensented in Sec. 4 and 5, respectively.

2. JT-60 ICRF Launching System and Test-stand

The design of the ICRF launcher of JT-60 was started from the beginning of 1984. We adopted the 2×2 phased loop antenna array, since we recognized the importance of phase control in optimization of the heating.

The coupling calculation was done to determine the dimension of the coupler with the three dimensional antenna coupling code [2,3].

A detailed mechanical and electrical design calculation was performed to satisfy the specifications imposed on the JT-60 launcher, which are summarized in Table 1. High power density, long pulse operation and disruptive instability were severe obstacles in establishment of the design. However, these points have been overcome by adopting pertinent mechanical structure and confirming it with three dimensional stress analysis.

Figure 1 shows the structure of the JT-60 ICRF launcher [1].

The fabrication of the launcher was completed in August, 1985. The other important components of the coupling system, such as stub tuners, DC breaks, directional couplers and U-links (trombones) have been also completed.

The total coupling system was assembled on the test stand before the installation into the JT-60 vacuum vessel. Figure 2 show the experimental set-up on the test stand. The vacuum vessel of 1300 ℓ capacity is evacuated with a turbo molecular pump of pumping speed 200 ℓ/s. Before the antenna conditioning, the launcher and the vacuum vessel were baked at 200°C during 60 hours. The base pressure after the baking and before the antenna conditioning was 4×10^{-8} Torr (N_2) and it decreased to 2×10^{-8} Torr (N_2) after the antenna conditioning.

The temperature of the launching system was measured by 51 thermocouples. A double stub tuner was equipped for each antenna. Rf power transmitted into the launching system was measured by a directional coupler located between the stub tuner and a generator. Since antenna loading resistance is very small because of vacuum loading, a large reactive power is accumulated between the antenna and the stub tuner. The accumulated power was measured by a directional coupler located between the stub and the antenna.

A rating of the rf power source is as follows.

Frequency : 120 MHz

Rf power : 100 kW

Pulse width : 10 sec

Duty cycle : 1/15

Output of the power source was supplied to the two lines of the launcher through a two-way power divider. The rest of the lines were short-circuited near the junction with the stub tuner. The transmission lines were filled with SF_6 gas at 2 atomospheric pressure.

3. Impedance Matching

Before the assemblage of the total launching system, we measured the mutual coupling between the loop antennae. The results are shown in a matrix form,

$$\begin{bmatrix} P_{11} & P_{12} & P_{13} & P_{14} \\ P_{21} & P_{22} & P_{23} & P_{24} \\ P_{31} & P_{32} & P_{33} & P_{34} \\ P_{41} & P_{42} & P_{43} & P_{44} \end{bmatrix} = \begin{bmatrix} 0 & -6.6 & -19.9 & -14.3 \\ -6.6 & 0 & -14.6 & -19.9 \\ -19.9 & -14.6 & 0 & -6.5 \\ -14.3 & -19.9 & -6.5 & 0 \end{bmatrix} \text{ dB} \tag{1}$$

where P_{ij} ($i, j = 1 \sim 4$) is the normalized power coupled to the j-th loop when the power is supplied from the i-th loop. Numbering of the loops is shown in Fig. 1. Coupling between the poloidal pair is the strongest (-6.6 dB). Coupling between the toroidal pair is medium (-14.3 dB) and the cross coupling is the weakest (-19.9 dB). Symmetry of the loop array was found to be quite good.

In order to evaluate the antenna input impedance, we must take the mutual impedance into account. The mutual impedance Z_{ij} can be written in the form,

$$\begin{bmatrix} V_1 \\ V_2 \\ V_3 \\ V_4 \end{bmatrix} = \begin{bmatrix} Z_{11} & Z_{12} & Z_{13} & Z_{14} \\ Z_{21} & Z_{22} & Z_{23} & Z_{24} \\ Z_{31} & Z_{32} & Z_{33} & Z_{34} \\ Z_{41} & Z_{42} & Z_{43} & Z_{44} \end{bmatrix} \begin{bmatrix} I_1 \\ I_2 \\ I_3 \\ I_4 \end{bmatrix} \tag{2}$$

where V_i and I_i ($i = 1 \sim 4$) are respectively voltage and current at the terminal point of each loop antenna. Antenna input impedance Z_{Ai} is defined as $Z_{Ai} = \frac{V_i}{I_i}$.

Using Eq. (2), we obtain

$$Z_{Ai} = \sum_{j=1}^{4} Z_{ij} \cdot \frac{I_j}{I_i} \quad . \tag{3}$$

From the above relation, we can find that the antenna input impedance can be controlled by the choice of the current direction of each antenna, i.e. antenna phasing. The antenna input impedances for various phasing conditions are as follows.

$(0,\pi)$; $Z_{Ai} = Z_{i1} + Z_{i2} + Z_{i3} + Z_{i4}$

(π,π) ; $Z_{Ai} = Z_{i1} + Z_{i2} - Z_{i3} - Z_{i4}$

$(0,0)$; $Z_{Ai} = Z_{i1} - Z_{i2} - Z_{i3} + Z_{i4}$

$(\pi,0)$; $Z_{Ai} = Z_{i1} - Z_{i2} - Z_{i3} - Z_{i4}$

where (ψ,θ) means respectively toroidal and poloidal phase differences. The directions of the current for each case are illustrated as follows.

$(0,\pi)$	(π,π)	$(0,0)$	$(\pi, 0)$
↓ ↓ ↑ ↑	↓ ↑ ↑ ↓	↓ ↓ ↓ ↓	↓ ↑ ↓ ↑

The mutual inductance is the largest for $(0,\pi)$ and is the smallest for $(\pi,0)$.

The impedance matching of the 2×2 loop array was achieved with the stub tuners for various phasing conditions. Because of good symmetry of the antenna array, the stub positions necessary for the impedance matching are almost the same for all the lines. We can obtain impedance matching simply by scanning each stub tuner by almost equal length.

The input impedances of the antenna array with simultaneous injection into all the ports can be deduced from the stub matching positions. The results are indicated on the Smith chart in Fig. 3 for 120 MHz. As discussed above, the electric length becomes larger in order with $(\pi,0)$, $(0,0)$ and $(0,\pi)$.

It should be noted that the antenna input impedance can be changed considerably by phase control. It is important to calculate the antenna-plasma coupling, taking the mutual coupling between loops into

account. This work is now in progress for the 2 × 2 antenna array.

One should also note that the input impedance of the single loop operation, where the other lines are terminated with 50 Ω load, is near the quarter wavelength resonance, as shown in Fig. 3.

4. Multipactoring phenomena

Rf power was fed to one of the poloidal pairs (antennae I and II) through the two-way power divider with the phase difference of π, which means that the current directions of the antennae I and II coincide.

Positions of the stub tuners were controlled so that the power coupling to the antennae III and IV was small. Typical power partition among the loops were as follows.

$$P_I : P_{II} : P_{III} : P_{IV} = 1 : 0.98 : 0.14 : 0.53 \quad .$$

We observed strong multipactoring phenomena at low power region. Figure 4 shows the power dependence of the multipactoring discharge. The vertical axis is increase of gas pressure associated with the rf pulse. At about 10 kW, large increase of pressure was observed. Strong light due to the discharge was seen around the feedthrough of the antennae III and IV. The corresponding peak value of the voltage standing wave was less than ~7 kV.

The position of the discharge changes with the power. The light near the feedthrough moved to the antenna at 20 kW. At the power of 30 kW, the discharge took place inside the antenna casing, and the outgassing decreased. Above 40 kW, the discharge was not observed inside the launcher, and the outgassing was further reduced. Weak light was observed outside the launcher and hot spots were seen on the coil and the central conductors of the lines I and II. Number of the hot spot increases with the power, but the gas pressure was kept at the low level up to 100 kW.

The multipactoring discharge causes large reflection at the start and end phase of the rf pulse. Figure 5 (a) ~ (c) show the oscillograms of the incident voltage measured by the directional coupler located after the stub tuner and the incident and reflected voltages measured before the stub tuner. The rf power of each case is (a) 6.4 kW, (b) 12 kW and (c) 35 kW.

In Fig. 5(a), large reflected voltage was observed at the start of the pulse and reflected power increased gradually in the latter half of the pulse due to the onset of the multipactoring discharge. At the start of the pulse, we always encounter the forbidden band of the power due to the multipactoring phenomena. The ramp-up rate of the pulse must be as rapid as possible, otherwise the pulse is interrupted by the reflection alarm circuit.

In the interm diate power region, the pulse was noisy but its amplitude became constant except at the start of the pulse as shown in Fig. 5(b). In the high power region (Fig. 5(c)), the pulse became stable and the mismatching at the start of the pulse was reduced. Above this power, we could easily increase the rf power up to the maximum power of the generator.

5. Observation of Aging Process

The aim of this power test is to inject the rf power of 100 kW during 10 sec into the launching system. Therefore we increased the pulse width step by step up to 10 sec, monitoring the power accumulated in the launching system, the temperature at various points of the launcher and the pressure in the vacuum vessel.

The power level of the aging was 60 ~ 100 kW, so that the multipactoring discharge was suppressed inside the launcher. In this power region, we observed the hot spots on the central conductor and the weak light outside the launcher as described in Sec. 4.

Figure 6 shows the gas pressure during the rf pulse P_G versus rf energy W. It is found that the aging was in progress day by day. P_G increases non-linearly with W. A large jump of P_G was seen at 1 MJ. This might be due to insufficiency of aging time.

The temperature of the launcher was measured at various positions of the launcher i.e. the Faraday shield, the guard limiter, the coaxial lines (outer conductor), the feedthrough (outer conductor) and so on. The highest rise of the temperature was detected at the gap of the guard limiter. The rise of the temperature at this position, ΔT_{bulk}, is plotted as a function of W in Fig. 7. It is shown that ΔT_{bulk} is proportional with W and that there is no difference between the data of 27/9 and 28/9 in contrast with the relation between P_G and W (Fig.6).

This result indicates that the increase of the temperature was not due to anormalous discharge on the surface of the launcher but simply due to the joule loss on it.

The mechanism of the gas desorption associated with the rf pulse has not yet been made clear. It is not likely, however, that the

discharge phenomena play an important role in the gas desorption at least in the present aging process, since we avoided the power region of the multipactoring discharge.

From the mass analysis of the desorbed gas, increase of hydrogen was found to be the most prominent. Secondly CO increased largely. Figure 8 (a) and (b) show the data of the mass analysis. It is a feature of the rf aging that H_2O does not increase. Similar tendency was seen for much higher frequency case in JAERI (2 GHz, lower hybrid range of frequency).

The aging process is shown in Figure 9. The abscissa is the integrated value of the injected energy from the start of the aging. The vertical axis is the gas pressure normalized by the rf power and the pulse width. 1 MJ injection was achieved after the aging of the total injection energy of ~45 MJ during two days.

The gas desorption rate at 1 MJ injection was 0.02 Torr·ℓ/s, which is at least two order of magnitude smaller than the value which affects the particle balance of JT-60. If the maximum power were injected, the gas desorption would further increase only by one order. Therefore the gas desorption from the launcher itself might be no problem.

Typical waveforms of 1 MJ injection are shown in Fig. 10 (a) ~ (d). Power is injected into the lines I and II. Incident and reflected power of them, P_{in} and P_{ref}, are shown in Fig. 10 (a). The power accumulated in the launching system P_{Ain}, which was measured with the directional couplers placed between the antenna and the stub tuners, are shown in Fig. 10 (b). These signals are of forward wave. The voltage standing wave ratio (VSWR) of the launching system is quite high because of the vacuum loading. Then, the coupling resistance R_c and the maximum voltage of the launching system V_{Max} are given as follows.

$$R_c \simeq Z_0 \cdot \frac{P_{in} - P_{ref}}{4 P_{Ain}}$$

$$V_{Max} \simeq 2\sqrt{2 Z_0 P_{Ain}} \quad ,$$

where Z_0 is a characteristic impedance of the coaxial lines of the launching system. Temporal change of R_c and V_{Max} are illustrated in Fig. 10 (c) and (d), respectively. Besides the early phase of the pulse, R_c is almost constant. R_c is 0.35 Ω and 0.3 Ω for the antennae I and II, respectively. The small difference of R_c between I and II may be due to the subtle phase difference of the two lines from 180°. The averaged coupling resistance including the coupling to the lines III and IV, $\bar{R}_c$, is defined as

$$\bar{R}_c \simeq Z_0 \frac{\sum_{j=1}^{2} (P_{inj} - P_{refj})}{4 \sum_{j=1}^{4} P_{Ainj}}$$

$\bar{R}_c$ is 0.27Ω in this case. The relation between $\bar{R}_c$ and the resistance per unit length of the launching system, r_c, is

$$r_c \simeq \frac{2 \bar{R}_c}{L} \quad ,$$

where L is the total length of the launching system. Assuming the radiation resistance in the vacuum to be 0.1Ω and using L = 10.7 m, r_c is 0.031 Ω/m. This value is consistent with the design value of the 6 inch coaxial lines at 120 MHz and room temperature.

V_{Max} of I and II is 28 kV and 26 kV, respectively. These are about 50% of the maximum rating of the JT-60 ICRF launcher. The energy loss of 1 MJ per two lines is also about 50% of the maximum rating.

6. Conclusions

Impedance matching and power test of the JT-60 ICRF launching system was performed on the test stand before the installation into JT-60. Following results were obtained.

1. Impedance matching of 2×2 loop antenna in vacuum was investigated with various phasing. Input impedance of the loop antennae changes considerably with phasing due to the strong mutual coupling.
2. Intense multipactoring discharge was observed only at the low power level, i.e. for the voltage of standing wave less than ~7 kV.
3. 1 MJ has been injected into the half part of the launcher. Gas production rate can be suppressed at modest value ($\sim 10^{-2}$ Torr·ℓ/s) after some aging process.
4. Desorbed gas is mainly hydrogen.
5. Coupling resistance in the vacuum is 0.3 ~ 0.35 Ω, which is consistent with the estimation of the resistance of the launching system.

Acknowledgements

We would like to thank Drs. T. Nagashima and H. Shirakata for their encouragements. Thanks are also due to the other members of Plasma Heating Laboratory II and RF Group of Heating System Development Division of JAERI for their supports.

References

[1] NAGASHIMA, T., UEHARA, K., KIMURA, H., et al., "JT-60 Radio-Frequency Heating System Descriptions and R & D Results", to be published in Nuclear Engineering and Design/Fusion.

[2] KIMURA, H., FUJII, T., IKEDA, Y., et al., Proc. of the 4th Joint Varenna-Grenoble Int. Symp. on Heating in Toroidal Plasmas, Vol. II, P. 1128, Rome, Italy, Mar., 1984.

[3] IKEDA, Y., KIMURA, H., FUJII, T., et al., Japan Atomic Energy Research Institute Report, JAERI-M 84-191 (in Japaneses) (1984).

Acknowledgements

We would like to thank Drs. T. Nagashima and H. Shirakata for their encouragements. Thanks are also due to the other members of Plasma Heating Laboratory II and RF Group of Heating System Development Division of JAERI for their supports.

References

[1] NAGASHIMA, T., UEHARA, K., KIMURA, H., et al., "JT-60 Radio-Frequency Heating System Descriptions and R & D Results", to be published in Nuclear Engineering and Design/Fusion.

[2] KIMURA, H., FUJII, T., IKEDA, Y., et al., Proc. of the 4th Joint Varenna-Grenoble Int. Symp. on Heating in Toroidal Plasmas, Vol. II, P. 1128, Rome, Italy, Mar., 1984.

[3] IKEDA, Y., KIMURA, H., FUJII, T., et al., Japan Atomic Energy Research Institute Report, JAERI-M 84-191 (in Japaneses) (1984).

JT-60 ICRF Launcher Specifications

Table 1

1. 2×2 Phased Loop Antenna Array
2. Faraday Shield
   - Arch shape
   - Open type (gap/pitch=0.5)
   - Material : Inconel
   - Coating : Cu+TiC
3. Guard Limiter
   - Material : Molibdenum
   - Coating : TiC
4. Feedthrough
   - Two-stage
5. Baking Temperature
   - 250℃
6. Electric and Thermal Coditions

RF power :	6MW
VSWR :	25
Pulse Length :	10 sec
Duty :	1/60
Total RF loss :	430kW
Heat flux from the plasma :	70kW

7. Mechanical Condition
   - Current quench time of disruption
     1 ms at 2.7MA

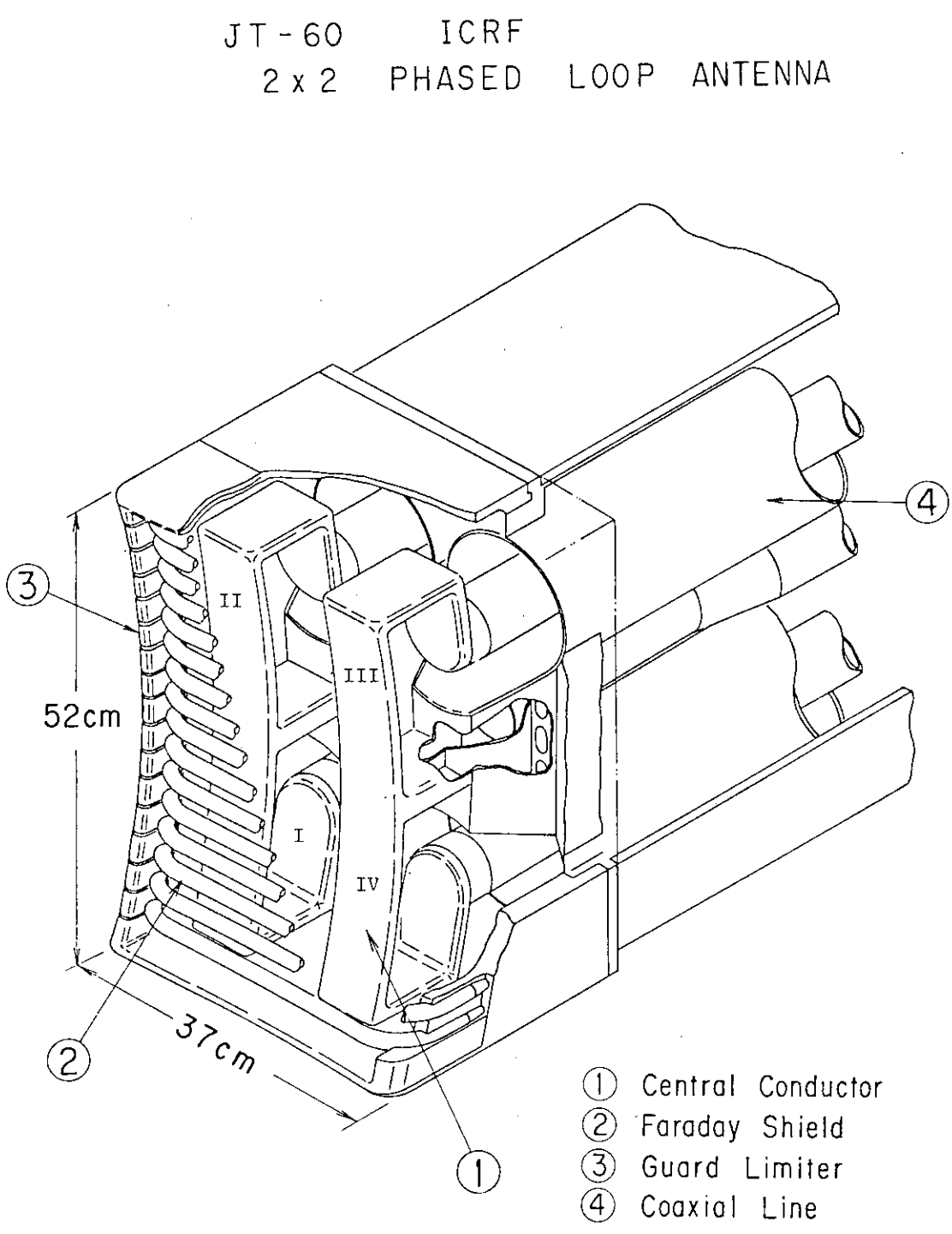

Fig. 1 Structure of the JT-60 ICRF 2×2 phased loop antenna array.

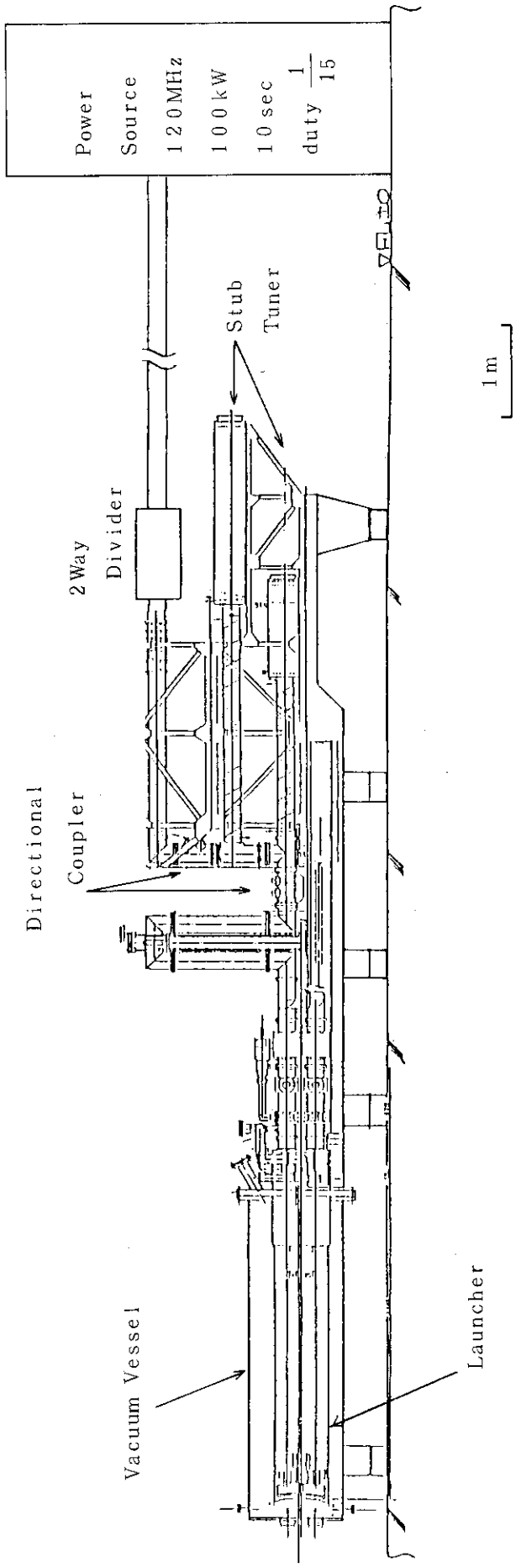

Fig. 2 Setup for the power test of the JT-60 ICRF launching system.

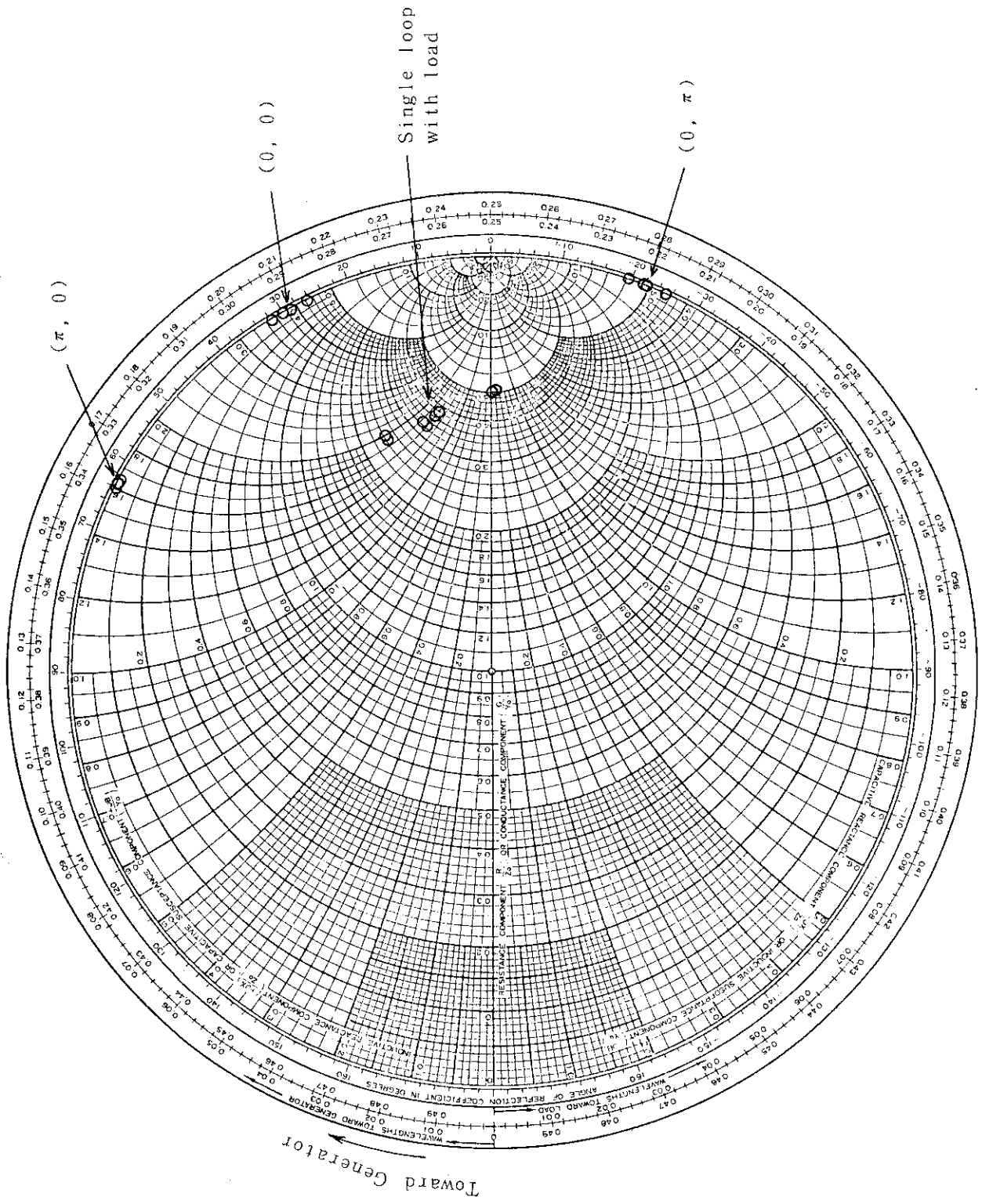

Fig. 3 Antenna input impedance for various phasing conditions, indicated on the Smith chart.

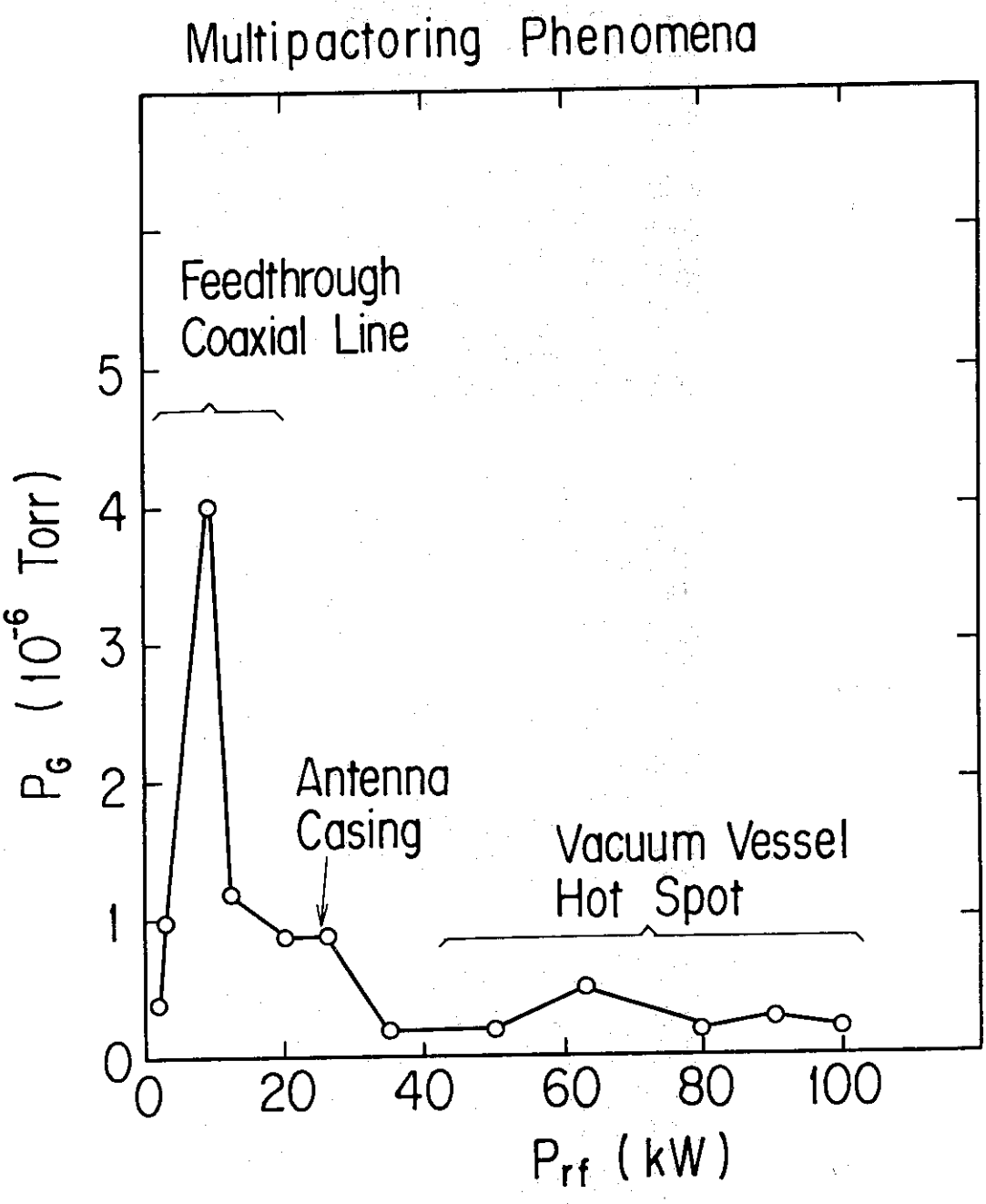

Fig. 4 Variation of the pressure in the vacuum vessel as a function of the rf power. Location where the multipactoring discharge took place is shown in the figure.

(a)

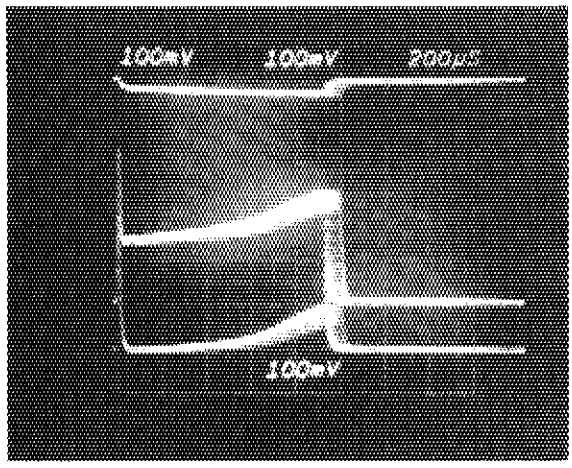

(b)

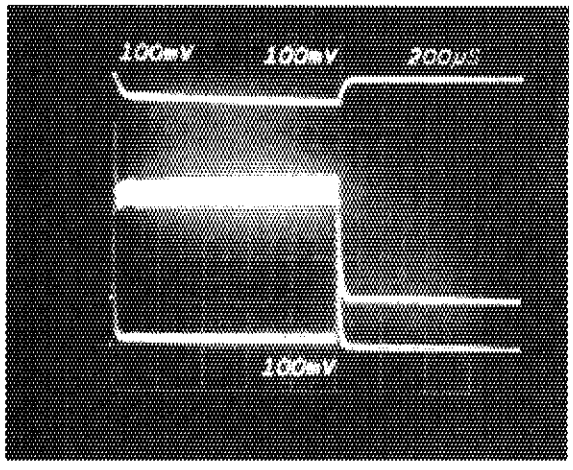

(c)

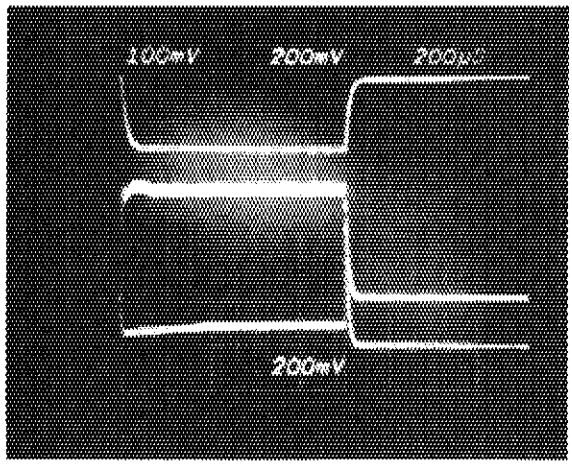

Fig. 5 Waveforms of the incident voltage measured after the stub tuner (upper trace), incident and reflected voltages measured before the stub tuner (middle and lower traces, respectively). Rf power is (a) 6.4 kW, (b) 12 kW and (c) 35 kW.

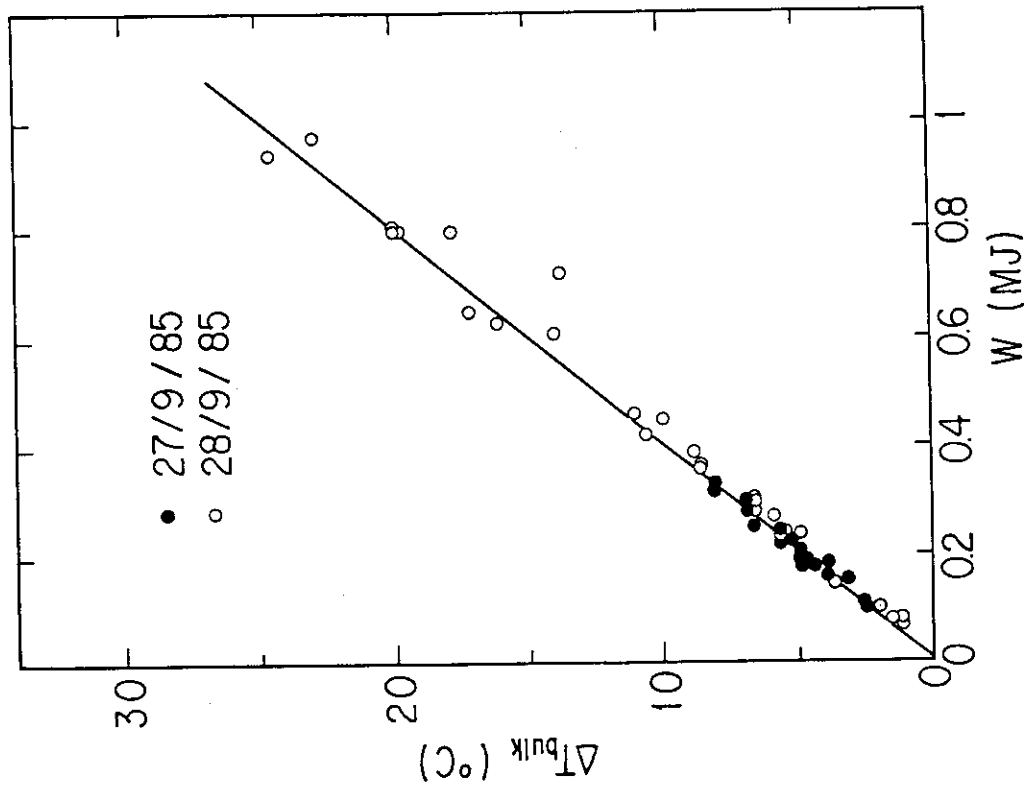

Fig. 7 Relation between the increment of the temperature at the gap of the guard limiter ΔT_{bulk} and the rf injection energy W.

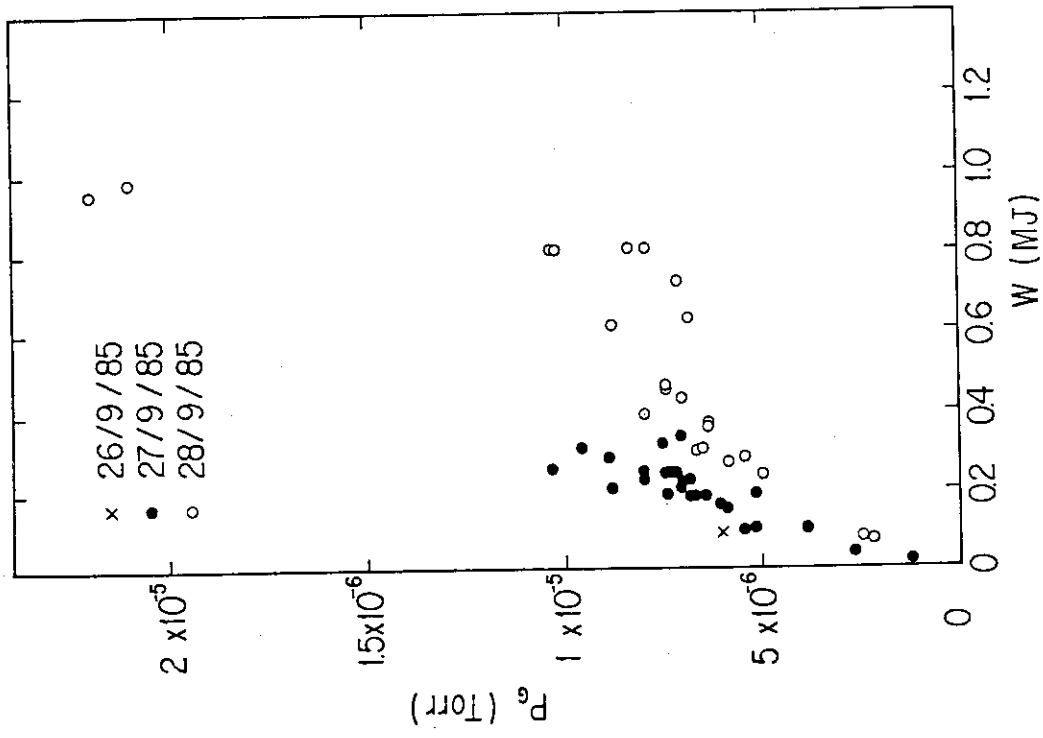

Fig. 6 Pressure in the vacuum vessel during rf pulse versus rf injection energy.

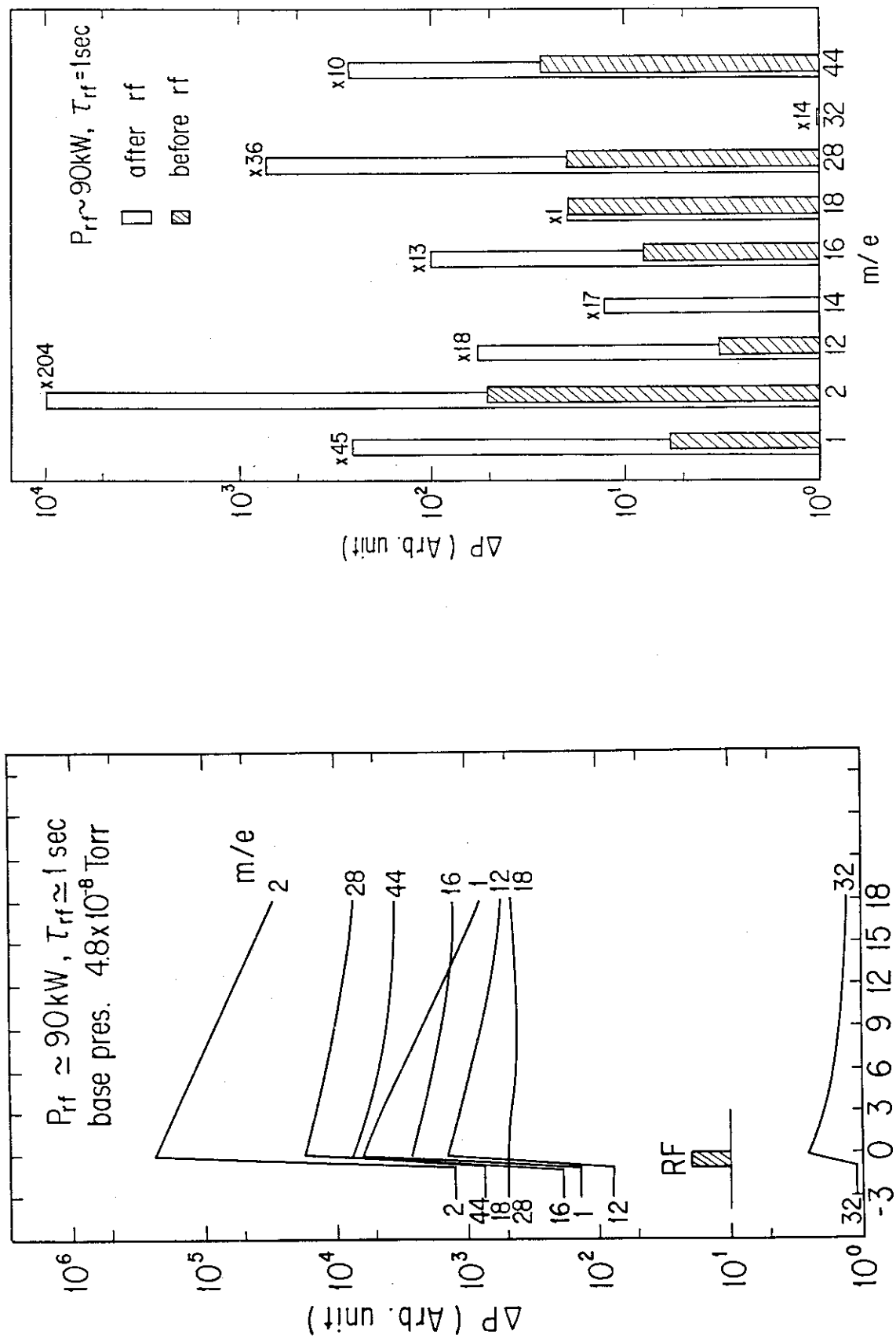

Fig. 8 Data of the mass analysis of the desorbed gas. (a) Time variation of the partial pressure of various mass number. (b) Ratio of the partial pressure after and before rf pulse.

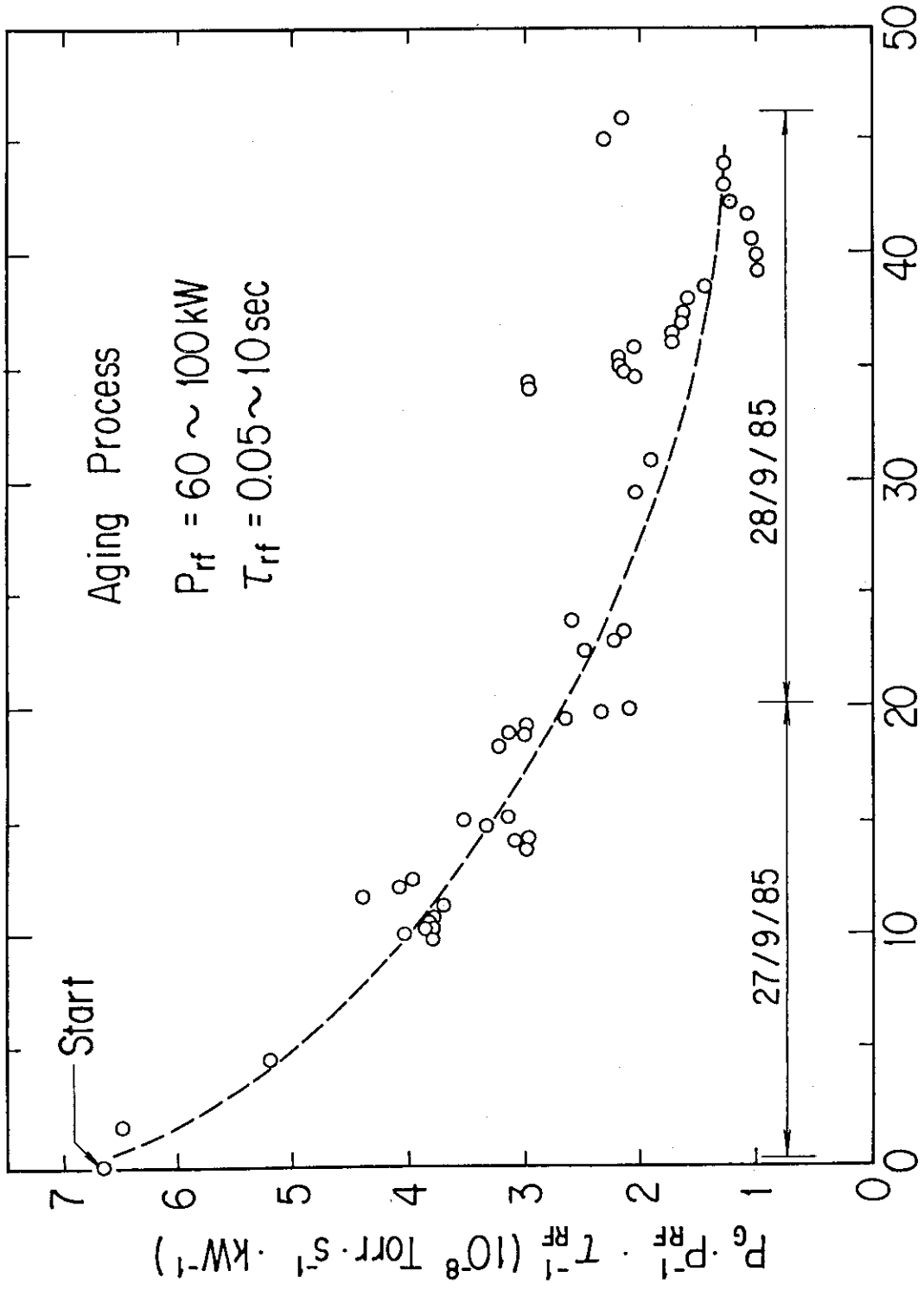

Fig. 9 Aging process. The vertical axis is the pressure normalized with the rf power and the pulse width. The abscissa is the integrated value of the injected energy from the start of the aging.

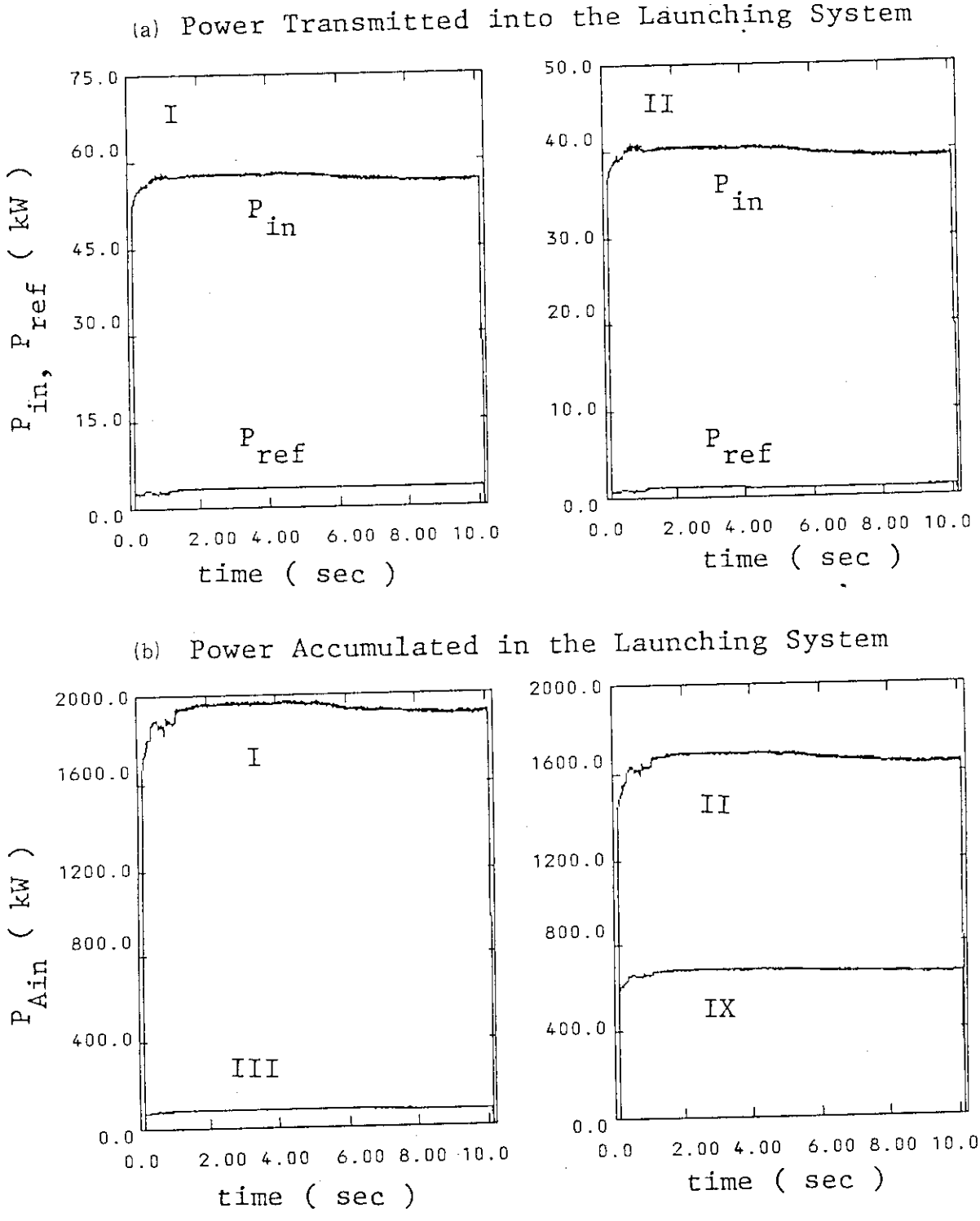

Fig. 10 Waveforms of 1 MJ injection. (a) Power transmitted into the launching system. (b) Power accumulated in the launching system. (c) Loading resistance in the vacuum. (d) Maximum voltage generated in the launching system.

(c) Loading Resistance in the Vacuum

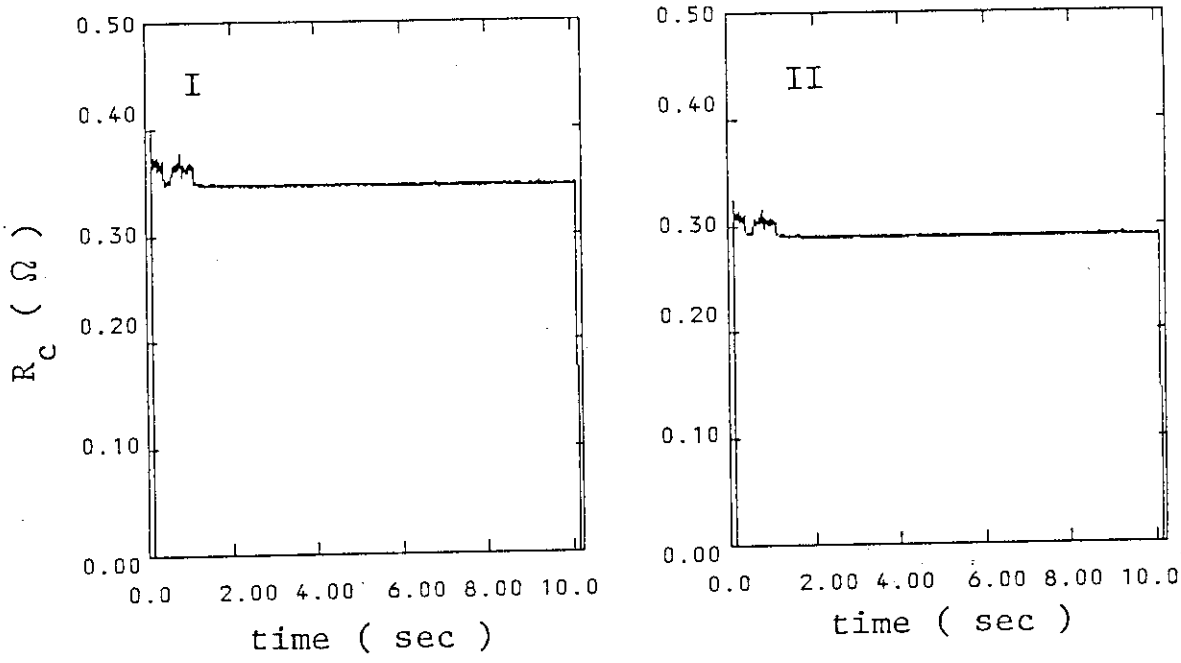

(d) Maximum Voltage in the Launching System

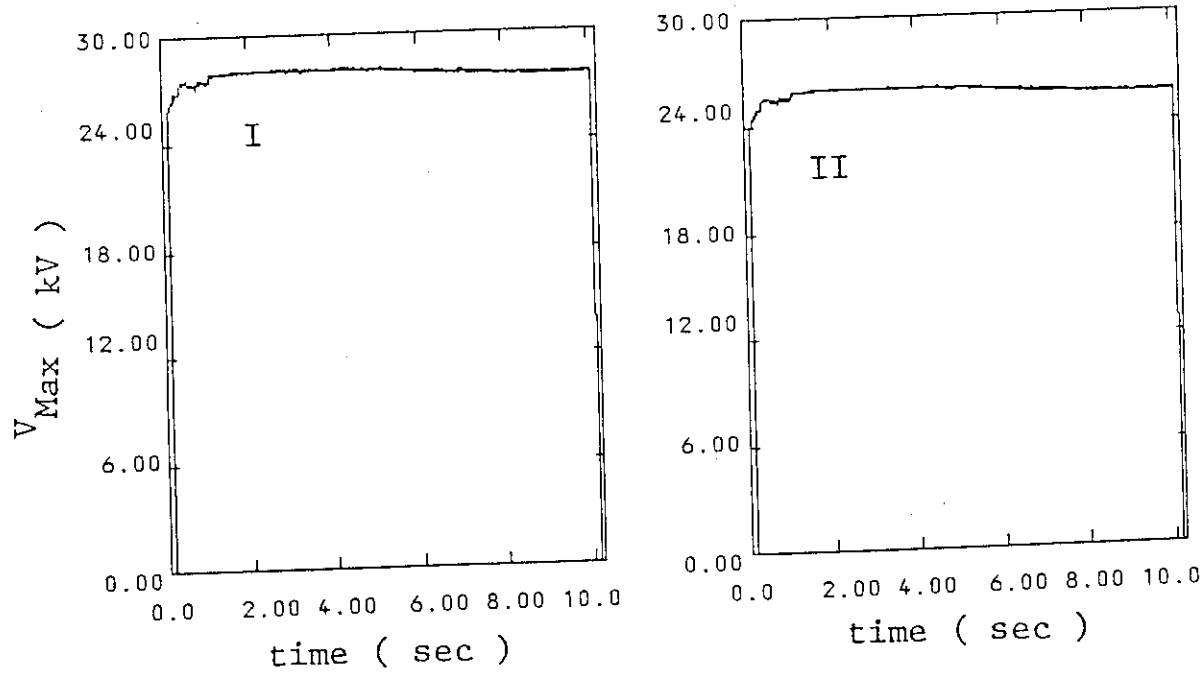

Fig. 10 (Con'd)